

## Metal-Centered Ferrocene Clusters from 5-Ferrocenylpyrimidine and Ferrocenylpyrazine

Ryo Horikoshi,<sup>†</sup> Chisato Nambu, and Tomoyuki Mochida\*

Department of Chemistry, Faculty of Science, Toho University, Miyama, Funabashi, Chiba 274-8510, Japan

Received June 17, 2003

A series of metal-centered ferrocene compounds has been designed by using 5-ferrocenylpyrimidine (**L1**) and ferrocenylpyrazine (**L2**). These ligands, when combined with transition metal salts, produce mixed-metal polynuclear complexes with structural diversity. Reaction of **L1** with  $M(\text{SCN})_2$  ( $M = \text{Ni}, \text{Co}$ ) produces the pinwheel-like 4:1 complexes  $(\text{L1})_4 \cdot M(\text{SCN})_2$ , while reactions of **L1** and **L2** with  $\text{Cu}(\text{NO}_3)_2$  give the 3:1 complex  $(\text{L1})_3 \cdot \text{Cu}(\text{NO}_3)_2$  and the 2:1 complex  $(\text{L2})_2 \cdot \text{Cu}(\text{NO}_3)_2$ , respectively. Reactions of **L1** and **L2** with  $M(\text{hfac})_2$  ( $\text{hfac} = 1,1,1,5,5,5$ -hexafluoroacetylacetonate,  $M = \text{Mn}, \text{Ni}, \text{Cu}, \text{Zn}$ ) produce 2:1 complexes  $(\text{L2})_2 \cdot M(\text{hfac})_2$  with cis and trans configurations, respectively. Crystal structures as well as solid-state electrochemical properties of these redox active complexes were investigated.

### Introduction

The tailored construction of mixed-metal supramolecular assemblies, by complexation of organometallic ligands and transition metal ions, is receiving much attention associated with their characteristics such as redox, magnetic, optical, and electronic properties.<sup>1</sup> Various ferrocene-containing ligands have been synthesized to date, focusing on their well-behaved redox activity as well as their synthetic versatility.<sup>1b,2</sup> In particular, 1,1'-substitution of ferrocene with various donor heteroatoms has produced versatile ligands such as 1,1'-bis(diphenylphosphino)ferrocene (dppf); they often afford chelate complexes, although there are some interesting exceptions.<sup>1b,3,4</sup> We designed 1,1'-bis-pyridinethio-substituted ferrocenes, to produce bridging ligands rather than chelating ligands.<sup>5</sup> Recently, preparations of 1,1'-bis(4-pyridyl)ferrocene ((4-py)<sub>2</sub>fc)<sup>6</sup> and its analogues<sup>7</sup> have been reported; these act as a bridging ligand to produce metalla-macrocycles. On the other hand, however, only a few examples of monosubstituted ferrocene-based bridging ligands have been reported to date.<sup>8</sup> Ferrocene carboxylate, for example, is a

highly versatile ligand, because it exhibits various bonding modes, producing interesting coordination compounds.<sup>9</sup> To explore the possibilities of monosubstituted ferrocenes to form novel molecular architectures, we have designed 5-ferrocenylpyrimidine (**L1**) and ferrocenylpyrazine (**L2**) (Scheme 1), which may act as bidentate ligands. The metal bridging abilities of pyrimidine and pyrazine moieties are well documented.<sup>10</sup> In a separate paper,<sup>11</sup> we have reported the preparation of side-chain coordination polymers based on

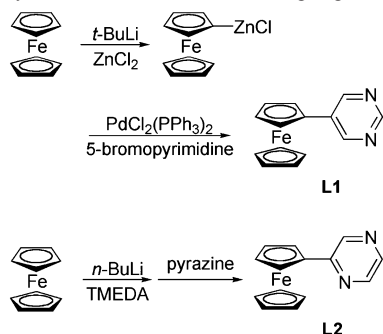
- (2) (a) Bradley, S.; Camm, K. D.; Liu, X.; McGowan, P. C.; Mumtaz, R.; Oughton, K. A.; Podesta, T. J.; Thornton-Pett, M. *Inorg. Chem.* **2002**, *41*, 715–726. (b) Chandrasekhar, V.; Nagendran, S.; Bansal, S.; Cordes, A. W.; Vij, A. *Organometallics* **2002**, *21*, 3297–3300. (c) Lindner, E.; Ayasse, C. S.; Eichele, K.; Steimann, M. *Organometallics* **2002**, *21*, 4217–4225. (d) Adams, R. D.; Qu, B.; Smith, M. D. *Organometallics* **2002**, *21*, 3867–3872. (e) Gibson, V. C.; Long, N. J.; White, A. J. P.; Williams, C. K.; Williams, D. J. *Organometallics* **2002**, *21*, 770–772. (f) Yip, J. H. K.; Wu, J.; Wong, K.-Y.; Yeung, K.-W.; Vittal, J. J. *Organometallics* **2002**, *21*, 1612–1621. (g) Herberhold, M. *Angew. Chem., Int. Ed.* **2002**, *41*, 956–958. (h) Ion, A.; Moutet, J.-C.; Saint-Aman, E.; Royal, G.; Gautier-Luneau, I.; Bonin, M.; Ziessel, R. *Eur. J. Inorg. Chem.* **2002**, 1357–1366. (i) Shafir, A.; Fiedler, D.; Arnold, J. J. *Chem. Soc., Dalton Trans.* **2002**, 555–560. (j) Gibson, V. C.; Long, N. J.; White, A. J. P.; Williams, C. K.; Williams, D. J.; Fontani, M.; Zanello, P. J. *Chem. Soc., Dalton Trans.* **2002**, 3280–3289. (k) André-Bentabet, E.; Broussier, R.; Amardeil, R.; Hierro, J.-C.; Richard, P.; Fasseur, D.; Gautheron, B.; Meunier, P. J. *Chem. Soc., Dalton Trans.* **2002**, 2322–2327. (l) Canales, S.; Crespo, O.; Fortea, A.; Gimeno, M. C.; Jones, P. G.; Laguna, A. J. *Chem. Soc., Dalton Trans.* **2002**, 2250–2255. (m) Štěpnička, P. *New J. Chem.* **2002**, *26*, 567–575. (n) Štěpnička, P.; Čiśařová, I. *New J. Chem.* **2002**, *26*, 1389–1396. (o) Troitskaya, L. L.; Ovseenko, S. T.; Slovokhotov, Y. L.; Neretin, I. S.; Sokolov, V. I. *J. Organomet. Chem.* **2002**, *642*, 191–194. (p) Long, N. J.; White, A. J. P.; Williams, D. J.; Younus, M. J. *Organomet. Chem.* **2002**, *649*, 94–99.

\* To whom correspondence should be addressed. E-mail: mochida@chem.sci.toho-u.ac.jp.

<sup>†</sup> Present address: School of Science and Technology, Kwansei Gakuin University, Gakuen, Sanda, Hyogo, 669-1337 Japan.

(1) (a) *Supramolecular Organometallic Chemistry*; Haiduc, I., Edelmann, F. T., Eds.; Wiley-VCH: Weinheim, 1999. (b) *Ferrocenes: Homogeneous Catalysis, Organic Synthesis, Material Science*; Togni, A., Hayashi, T., Eds.; Wiley-VCH: Weinheim, 1995. (c) Long, N. J. *Metalloenes: An Introduction to Sandwich Complexes*; Blackwell Science Inc.: Cambridge, MA, 1998. (d) Braga, D.; Grepioni, F.; Desiraju, G. R. *Chem. Rev.* **1998**, *98*, 1375–1405.

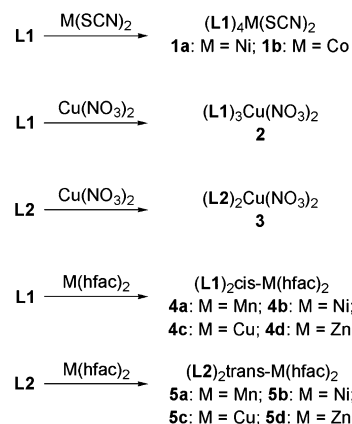
Scheme 1. Syntheses of Ferrocene-Containing Ligands



**L1**, in which the ligand acts as a bidentate one. In this study, we have prepared a series of metal-centered molecular complexes, in which the ligands act as monodentate ones.

- (3) (a) Bandoli, G.; Dolmella, A. *Coord. Chem. Rev.* **2000**, *209*, 161–196. (b) Choi, N.-S.; Lee, S. W. *J. Organomet. Chem.* **2001**, *627*, 226–232. (c) Gimeno, M. C.; Jones, P. G.; Laguna, A.; Sarroca, C.; Villacampa, M. D. *Inorg. Chim. Acta* **2001**, *316*, 89–93. (d) Maisela, L. L.; Crouch, A. M.; Darkwa, J.; Guzei, I. A. *Polyhedron* **2001**, *20*, 3189–3200. (e) Zhuravel, M. A.; Moncarz, J. R.; Glueck, D. S.; Lam, K.-C.; Rheingold, A. L. *Organometallics* **2000**, *19*, 3447–3454. (f) Canales, S.; Crespo, O.; Gimeno, M. C.; Jones, P. G.; Laguna, A. *J. Organomet. Chem.* **2000**, *613*, 50–55. (g) Gimeno, M. C.; Jones, P. G.; Laguna, A.; Sarroca, C. *J. Organomet. Chem.* **2000**, *596*, 10–15. (h) Gimeno, M. C.; Jones, P. G.; Laguna, A.; Sarroca, C. *J. Chem. Soc., Dalton Trans.* **1998**, 1277–1280. (i) Canales, F.; Gimeno, M. C.; Jones, P. G.; Laguna, A.; Sarroca, C. *Inorg. Chem.* **1997**, *36*, 5206–5211. (j) Canales, F.; Gimeno, M. C.; Laguna, A.; Jones, P. G. *J. Am. Chem. Soc.* **1996**, *118*, 4839–4845.
- (4) Houlton, A.; Mingos, D. M. P.; Murphy, D. M.; Williams, D. J.; Phang, L.-T.; Hor, T. S. A. *J. Chem. Soc., Dalton Trans.* **1993**, 3629–3630.
- (5) Horikoshi, R.; Mochida, T.; Moriyama, H. *Inorg. Chem.* **2002**, *41*, 3017–3024.
- (6) Braga, D.; Polito, M.; Braccacini, M.; D'Addario, D.; Tagliavini, E.; Preserpio, D. M.; Grepioni, F. *Chem. Commun.* **2002**, 1080–1081.
- (7) Horikoshi, R.; Hagiwara, K.; Mochida, T., submitted.
- (8) (a) Gao, D.; Li, Y. T.; Duan, C. Y.; Mo, H.; Meng, Q. *J. Inorg. Chem.* **2003**, *42*, 2519–2530. (b) Hou, H.; Li, G.; Li, L.; Zhu, Y.; Meng, X.; Fan, Y. *Inorg. Chem.* **2003**, *42*, 428–435. (c) Cooke, M.; Cameron, T. S.; Robertson, K. N.; Swarts, J. C.; Aquino, M. A. S. *Organometallics* **2002**, *21*, 5962–5971. (d) Costa, R.; López, C.; Molins, E.; Espinosa, E. *Inorg. Chem.* **1998**, *37*, 5686–5689.
- (9) (a) Yang, Y.-Y.; Wong, W.-T. *Chem. Commun.* **2002**, 2716–2717. (b) Guo, D.; Mo, H.; Duan, C. Y.; Lu, F.; Meng, Q. *J. Chem. Soc., Dalton Trans.* **2002**, 2593–2594. (c) Christie, S. D.; Subramanian, S.; Thompson, L. K.; Zaworotko, M. J. *J. Chem. Soc., Chem. Commun.* **1994**, 2563–2564.
- (10) (a) Leininger, S.; Olenyuk, B.; Stang, P. J. *Chem. Rev.* **2000**, *100*, 853–908. (b) Munakata, M.; Wu, L.-P.; Kuroda-Sowa, T. *Adv. Inorg. Chem.* **1999**, *46*, 173–303. (c) Hagrman, P. J.; Hagrman, D.; Zubieta, J. *Angew. Chem., Int. Ed.* **1999**, *38*, 2638–2684. (d) Kitagawa, S.; Kondo, M. *Bull. Chem. Soc. Jpn.* **1998**, *71*, 1739–1753. (e) Munakata, M.; Wu, L.-P.; Kuroda-Sowa, T. *Bull. Chem. Soc. Jpn.* **1997**, *70*, 1727–1743. (f) Sharma, C. V. K.; Griffin, S. T.; Rogers, R. D. *Chem. Commun.* **1998**, 215–216. (g) Lloret, F.; De Munno, G.; Julve, M.; Cano, J.; Ruiz, R.; Caneschi, A. *Angew. Chem., Int. Ed.* **1998**, *37*, 135–138. (h) Keller, W. S. *Angew. Chem., Int. Ed. Engl.* **1997**, *36*, 247–248. (i) Dong, Y.-B.; Smith, M. D.; Layland, R. C.; zur Loye, H.-C. *Inorg. Chem.* **1999**, *38*, 5027–5033. (j) Ezuhara, T.; Endo, K.; Aoyama, Y. *J. Am. Chem. Soc.* **1999**, *121*, 3279–3283. (k) Ezuhara, T.; Endo, K.; Hayasida, O.; Aoyama, Y. *New J. Chem.* **1998**, 183–188. (l) Ezuhara, T.; Endo, K.; Matsuda, K.; Aoyama, Y. *New J. Chem.* **2000**, *24*, 609–613. (m) Omata, J.; Ishida, T.; Hashizume, D.; Iwasaki, F.; Nogami, T. *Inorg. Chem.* **2001**, *40*, 3954–3958. (n) Riggio, I.; van Albada, G. A.; Ellos, D. D.; Spek, A. L.; Reedijk, J. *Inorg. Chim. Acta* **2001**, *313*, 120–124. (o) Ishida, T.; Kawakami, T.; Mitsubori, S.; Nogami, T.; Yamaguchi, K.; Iwamura, H. *J. Chem. Soc., Dalton Trans.* **2002**, 3177–3186. (p) Beauchamp, D. A.; Loeb, S. J. *Chem. Commun.* **2002**, 2484–2485. (q) Rossenbeck, B.; Sheldrick, W. S. *Z. Naturforsch.* **1999**, *54b*, 1510–1516. (r) Kromp, T.; Sheldrick, W. S. *Z. Naturforsch.* **1999**, *54b*, 1175–1180.
- (11) Horikoshi, R.; Ueda, M.; Mochida, T. *New J. Chem.* **2003**, *27*, 933–937.

Scheme 2. General Reaction Scheme



This paper describes the preparation, structures, and electrochemical properties of **L1**, **L2**, and their polynuclear metal complexes,  $(\mathbf{L1})_4\cdot\text{M}(\text{SCN})_2$  ( $\text{M} = \text{Ni}$  (**1a**),  $\text{Co}$  (**1b**)),  $(\mathbf{L1})_3\cdot\text{Cu}(\text{NO}_3)_2$  (**2**),  $(\mathbf{L2})_2\cdot\text{Cu}(\text{NO}_3)_2$  (**3**), and  $(\mathbf{L2})\cdot\text{M}(\text{hfac})_2$  ( $\text{L} = \mathbf{L1}$ ,  $\text{M} = \text{Mn}$  (**4a**),  $\text{Ni}$  (**4b**),  $\text{Cu}$  (**4c**),  $\text{Zn}$  (**4d**);  $\text{L} = \mathbf{L2}$ ,  $\text{M} = \text{Mn}$  (**5a**),  $\text{Ni}$  (**5b**),  $\text{Cu}$  (**5c**),  $\text{Zn}$  (**5d**),  $\text{hfac} = 1,1,1,5,5,5$ -hexafluoroacetylacetonate) (Scheme 2), which can be regarded as electroactive ferrocene clusters. Ferrocene can work as an electron reservoir, and its metal-assisted assembly is highly intriguing in terms of molecular quantum devices, as demonstrated by G. J. Long in a cobalt complex containing four ferrocenes.<sup>12</sup> This study demonstrates that **L1** and **L2** are highly versatile ligands for synthesizing ferrocene-based metal assemblies.

## Experimental Section

**General Procedure and Chemicals.** All reagents and solvents were commercially available except for  $\text{PdCl}_2(\text{PPh}_3)_2$ , which was synthesized by following the literature procedure.<sup>13</sup> NMR spectra were recorded on a JEOL JNM-ECL-400 spectrometer. Infrared spectra were recorded on a JASCO FT-IR 230 spectrometer as KBr pellets. Cyclic voltammograms were recorded with an ALS/chi electrochemical analyzer model 600A. Solution state measurements were performed in dichloromethane solutions containing 0.1 mol  $\text{dm}^{-3}$   $n\text{Bu}_4\text{NClO}_4$  as the supporting electrolyte, at a scan rate of 0.1  $\text{V s}^{-1}$ . A  $\text{Ag}/\text{Ag}^+$  reference electrode and a working electrode of a glassy carbon disk were used. Solid-state voltammograms were measured with a carbon-paste working electrode; well-ground mixtures of each bulk sample and carbon paste (graphite and mineral oil) were set in a cavity on a Teflon rod and connected to a platinum wire.<sup>5,14</sup> A three-electrode system was used with a platinum-wire counter electrode and a  $\text{Ag}/\text{AgCl}$  reference electrode, in 0.1 mol  $\text{dm}^{-3}$   $\text{NaClO}_4$  aqueous solutions at a scan rate of 0.1  $\text{V s}^{-1}$ , in the range  $-0.3$  to  $0.8$  V. Elemental analysis was performed on a Perkin-Elmer 2400CHN elemental analyzer.

**X-ray Diffraction Studies.** X-ray diffraction data for single crystals were collected on a Rigaku AFC-5S four-circle diffractometer equipped with a graphite crystal and incident beam mono-

- (12) Jiao, J.; Long, G. J.; Grandjean, F.; Beatty, A. M.; Fehner, T. P. *J. Am. Chem. Soc.* **2003**, *125*, 7522–7523.
- (13) Michelin, R. A.; Zanutto, L.; Braga, D.; Sabatino, P.; Angelici, R. J. *Inorg. Chem.* **1988**, *27*, 85–92.
- (14) (a) Noro, S.; Kondo, M.; Ishii, T.; Kitagawa, S.; Matsuzaka, H. *J. Chem. Soc., Dalton Trans.* **2002**, 3177–3186. (b) Kondo, M.; Shimamura, M.; Noro, S.; Kimura, Y.; Uemura, K.; Kitagawa, S. *J. Solid State Chem.* **2000**, *152*, 113–119.

**Table 1.** Crystallographic Data for **L1**, **L2**, **1a**, **1b**, **2**, and **3**

	<b>L1</b>	<b>L2</b>	<b>1a</b>	<b>1b</b>	<b>2</b>	<b>3</b>
chemical formula	C <sub>14</sub> H <sub>12</sub> N <sub>2</sub> Fe	C <sub>14</sub> H <sub>12</sub> N <sub>2</sub> Fe <sub>2</sub>	C <sub>58</sub> H <sub>48</sub> N <sub>6</sub> S <sub>2</sub> NiFe <sub>4</sub>	C <sub>58</sub> H <sub>48</sub> N <sub>6</sub> S <sub>2</sub> CoFe <sub>4</sub>	C <sub>42</sub> H <sub>36</sub> N <sub>8</sub> O <sub>6</sub> Fe <sub>3</sub> Cu	C <sub>28</sub> H <sub>24</sub> N <sub>6</sub> O <sub>6</sub> CuFe <sub>2</sub>
<i>a</i> /Å	6.897(4)	5.900(2)	11.348(3)	11.36(1)	13.455(3)	10.243(4)
<i>b</i> /Å	9.911(2)	20.141(2)	12.670(3)	12.63(1)	13.841(3)	7.820(3)
<i>c</i> /Å	16.868(3)	9.680(3)	9.152(1)	9.18(1)	13.350(5)	17.913(3)
$\alpha$ /deg			93.98(1)	93.8(1)	96.31(3)	
$\beta$ /deg	95.04(3)	98.40(3)	94.77(2)	94.8(1)	106.65(3)	105.02(2)
$\gamma$ /deg			81.08(2)	80.7(1)	119.14(2)	
<i>V</i> /Å <sup>3</sup>	1148.5(7)	1137.9(6)	1293.2(5)	1295(3)	1986(1)	1385.8(8)
<i>Z</i>	4	4	1		2	2
fw	264.11	264.11	1175.27	1175.51	979.88	715.77
space group	<i>P</i> 2 <sub>1</sub> / <i>c</i> (No. 14)	<i>P</i> 2 <sub>1</sub> / <i>c</i> (No.14)	<i>P</i> 1̄ (No. 2)	<i>P</i> 1̄ (No. 2)	<i>P</i> 1̄ (No. 2)	<i>P</i> 2 <sub>1</sub> / <i>a</i> (No. 14)
$\rho_{\text{calcd}}/\text{g}\cdot\text{cm}^{-3}$	1.527	1.542	1.509		1.638	1.715
$\mu/\text{cm}^{-1}$	12.87	12.99	15.77		16.61	18.48
<i>R</i> <sub>1</sub> <sup>a</sup>	0.041	0.035	0.047		0.070	0.039
<i>R</i> <sub>w</sub> <sup>a</sup>	0.120	0.123	0.108		0.117	0.130

$$^a R_1 = \sum ||F_o| - |F_c|| / \sum |F_o|; R_w = [\sum w(F_o^2 - F_c^2)^2 / \sum w(F_o^2)]^{1/2}.$$

**Table 2.** Crystallographic Data for **4b**, **4c**, **4d**, and **5c**

	<b>4b</b>	<b>4c</b>	<b>4d</b>	<b>5c</b>
chemical formula	C <sub>38</sub> H <sub>26</sub> N <sub>4</sub> O <sub>4</sub> F <sub>12</sub> Fe <sub>2</sub> Ni	C <sub>38</sub> H <sub>26</sub> N <sub>4</sub> O <sub>4</sub> F <sub>12</sub> CuFe <sub>2</sub>	C <sub>38</sub> H <sub>26</sub> N <sub>4</sub> O <sub>4</sub> F <sub>12</sub> Fe <sub>2</sub> Zn	C <sub>38</sub> H <sub>26</sub> N <sub>4</sub> O <sub>4</sub> F <sub>12</sub> CuFe <sub>2</sub>
<i>a</i> /Å	16.671(3)	16.848(3)	16.945(3)	11.747(5)
<i>b</i> /Å	13.222(2)	13.078(5)	13.016(3)	13.238(3)
<i>c</i> /Å	17.393(2)	17.521(5)	17.544(2)	6.447(2)
$\alpha$ /deg				96.47(2)
$\beta$ /deg	91.749(10)	92.25(2)	92.09(2)	93.04(3)
$\gamma$ /deg				78.49(2)
<i>V</i> /Å <sup>3</sup>	3832.0(8)	3857(1)	3866(1)	975.7(5)
<i>Z</i>	4	4	4	1
fw	1001.02	1005.87	1007.714	1005.87
space group	<i>C</i> 2/ <i>c</i> (No.15)	<i>C</i> 2/ <i>c</i> (No.15)	<i>C</i> 2/ <i>c</i> (No.15)	<i>P</i> 1̄ (No. 2)
$\rho_{\text{calcd}}/\text{g}\cdot\text{cm}^{-3}$	1.735	1.732	1.635	1.712
$\mu/\text{cm}^{-1}$	13.38	13.93	10.99	13.77
<i>R</i> <sub>1</sub> <sup>a</sup>	0.046	0.051	0.047	0.043
<i>R</i> <sub>w</sub> <sup>a</sup>	0.144	0.154	0.140	0.133

$$^a R_1 = \sum ||F_o| - |F_c|| / \sum |F_o|; R_w = [\sum w(F_o^2 - F_c^2)^2 / \sum w(F_o^2)]^{1/2}.$$

chromator using Mo K $\alpha$  radiation ( $\lambda = 0.71073$  Å) at 296 K. Crystal data, data collection parameters, and analysis statistics for **L1**, **L2**, **1a**, **1b**, **2**, **3**, **4b**, **4c**, **4d**, and **5c** are listed in Tables 1 and 2. Selected bond angles and bond lengths are given in Table 3. Powder X-ray measurements were performed on a Rigaku RAD-IIB. Compounds **1a–1b**, as well as **4a–4d** and **5a–5d**, were confirmed to be isomorphous by comparing X-ray diffraction patterns. All calculations were performed using the *teXsan* crystallographic software package.<sup>15</sup> These structures were solved by the direct method (SIR 92<sup>16</sup> and SHELEX 97<sup>17</sup>) and expanded using Fourier techniques. The non-hydrogen atoms were refined anisotropically, and absorption correction was applied ( $\psi$ -scan). The hydrogen atoms were inserted at the calculated positions and allowed to ride on their respective parent atoms.

Crystallographic data (excluding structure factors) for the structures reported in this paper have been deposited with the Cambridge Crystallographic Data Center as supplementary publication nos. CCDC 191982 (**L1**), CCDC 191983 (**L2**), CCDC 198073 (**1a**), CCDC 198074 (**2**), CCDC 198075 (**3**), CCDC 191985 (**4b**), CCDC 191986 (**4c**), CCDC 191987 (**4d**), and CCDC 191988 (**5c**). Copies of the data can be obtained free of charge on application to CCDC, 12 Union Road, Cambridge CB2 1EZ, U.K. (Fax: (+44)1223-336-033. E-mail: deposit@ccdc.cam.ac.uk.)

**5-Ferrocenylpyrimidine (L1).** A solution of ferrocene (1.1 g, 6.0 mmol) in THF (5 mL) was treated with a pentane solution of

*tert*-buthyllithium (1.6 M, 4.5 mL, 6.9 mmol) at 0 °C for 30 min. To this solution was added a suspension of anhydrous zinc chloride (1.0 g, 7.3 mmol) in THF (5 mL). The mixture was warmed to room temperature and stirred for 1 h to give zincated-ferrocene complex. To this mixture were added a suspension of PdCl<sub>2</sub>(PPh<sub>3</sub>)<sub>2</sub> (0.21 g, 0.3 mmol) in THF (10 mL) and then a solution of 5-bromopyrimidine (1.0 g, 6.1 mmol) in THF (10 mL). After being stirred for 24 h at room temperature, the mixture was treated with 2 M hydrochloric acid (2 mL). The reaction mixture was extracted with diethyl ether (100 mL) and washed with water (100 mL  $\times$  3). Then, the organic phase was dried over MgSO<sub>4</sub>. After evaporation of the solvent, the product was separated by column chromatography (silica gel, eluent: dichloromethane/diethyl ether = 9:1) to give **L1** in a 44% yield (0.68 g). Crystals of **L1** suitable for single-crystal X-ray analysis were obtained by slow evaporation of a pentane solution at ambient temperature. <sup>1</sup>H NMR (400 MHz, CDCl<sub>3</sub>, 25 °C, TMS, ppm)  $\delta$ : 9.04 (s, 1H), 8.81 (s, 2H), 4.70 (m, 2H), 4.45 (m, 2H), 4.10 (s, 5H). IR (KBr, cm<sup>-1</sup>): 3084 (w), 3022 (w), 1582 (m), 1556 (m), 1483 (m), 1438 (m), 1399 (s), 1293 (m), 1175 (m), 1138 (m), 1031 (m), 1007 (m), 888 (m), 842 (m), 813 (m), 722 (m), 512 (m), 495 (m), 467 (m). Anal. Calcd for C<sub>14</sub>H<sub>12</sub>N<sub>2</sub>Fe: C, 63.66; H, 4.58; N, 10.61. Found: C, 63.68; H, 4.26; N, 10.33.

**Ferrocenylpyrazine (L2).** A solution of pyrazine (3.6 g, 4.5  $\times$  10<sup>-2</sup> mol) in THF (50 mL) was added dropwise to a suspension of 1,1'-dilithioferrocene-tetramethylethylenediamine complex, prepared

(15) *teXsan: Crystal Structure Analysis Package*; Molecular Structure Corporation: The Woodlands, TX, 1985 and 1999.

(16) Altomare, A.; Cascarano, G.; Giacovazzo, C.; Guagliardi, A.; Burla, M. C.; Polidri, G.; Camalli, M. *J. Appl. Crystallogr.* **1994**, *27*, 435.

(17) Sheldrick, G. M. *Program for the Solution of Crystal Structures*; University of Göttingen: Göttingen, Germany, 1997.

**Table 3.** Selected Bond Lengths (Å) and Angles (deg) with Estimated Standard Deviations in Parentheses<sup>a</sup>

Complex 1a							
Ni–N(1)	2.1792(2)	Ni–N(3)	2.138(3)	Ni–N(5)	2.042(2)	N(1)–Ni–N(1) <sup>#1</sup>	180.0
N(1)–Ni–N(3)	87.27(9)	N(1)–Ni–N(3) <sup>#1</sup>	92.73(9)	N(1)–Ni–N(5)	89.93(9)	N(1)–Ni–N(5) <sup>#1</sup>	90.07(9)
N(3)–Ni–N(3) <sup>#1</sup>	180.0	N(3)–Ni–N(5)	89.56(10)	N(3)–Ni–N(5) <sup>#1</sup>	90.44(10)	N(5)–Ni–N(5) <sup>#1</sup>	180.0
Complex 2							
Cu–O(1)	1.987(3)	Cu–O(4)	1.979(3)	Cu–N(1)	2.276(4)	Cu–N(3)	2.035(3)
Cu–N(5)	2.036(3)	O(1)–Cu–O(4)	178.7(1)	O(1)–Cu–N(1)	90.6(1)	O(1)–Cu–N(3)	90.4(1)
O(1)–Cu–N(5)	91.3(1)	O(4)–Cu–N(1)	90.7(1)	O(4)–Cu–N(3)	89.6(1)	O(4)–Cu–N(5)	88.4(1)
N(1)–Cu–N(3)	101.3(1)	N(1)–Cu–N(5)	93.6(1)	N(3)–Cu–N(5)	165.1(1)		
Complex 3							
Cu–N(1)	1.976(4)	Cu–O(1)	2.007(3)	O(1)–Cu–O(1) <sup>#2</sup>	180.0	O(1)–Cu–N(1)	89.6(1)
O(1)–Cu–N(1) <sup>#2</sup>	90.4(1)	O(1) <sup>#2</sup> –Cu–N(1)	90.4(1)	O(1) <sup>#2</sup> –Cu–N(1) <sup>#2</sup>	89.6(1)	N(1)–Cu–N(1) <sup>#2</sup>	180.0
Complex 4b							
Ni–O(1)	2.047(3)	Ni–O(2)	2.012(3)	Ni–N(1)	2.102(4)	O(1)–Ni–O(1) <sup>#3</sup>	90.8(2)
O(1)–Ni–O(2)	88.7(1)	O(1)–Ni–O(2) <sup>#3</sup>	91.7(1)	O(1)–Ni–N(1)	88.7(1)	O(2)–Ni–N(1)	92.4(1)
Complex 4c							
Cu–O(1)	2.109(5)	Cu–O(2)	1.983(5)	Cu–N(1)	2.184(6)	O(1)–Cu–O(1) <sup>#4</sup>	92.0(3)
O(1)–Cu–O(2)	87.9(2)	O(1)–Cu–O(2) <sup>#4</sup>	92.5(2)	O(1)–Cu–N(1)	174.0(2)	O(2)–Cu–N(1)	86.2(2)
Complex 4d							
Zn–O(1)	2.104(3)	Zn–O(2)	2.064(2)	Zn–N(1)	2.174(3)	O(1)–Zn–O(1) <sup>#5</sup>	91.9(2)
O(1)–Zn–O(2)	85.76(10)	O(1)–Zn–O(2) <sup>#5</sup>	93.3(1)	O(1)–Zn–N(1)	171.6(1)	O(2)–Zn–N(1)	85.8(1)
Complex 5c							
Cu–O(1)	2.301(3)	Cu–O(2)	1.964(2)	Cu–N(1)	2.051(3)	O(1)–Cu–O(1) <sup>#1</sup>	180
O(1)–Cu–O(2)	86.37(9)	O(1)–Cu–O(2) <sup>#1</sup>	93.63(9)	O(1)–Cu–N(1)	94.7(1)	O(2)–Cu–N(1)	89.39(9)

<sup>a</sup> Symmetry codes used for generating equivalent atoms: <sup>#1</sup>,  $-x + 2, -y, -z + 2$ ; <sup>#2</sup>,  $-x + 1, -y + 1, -z$ ; <sup>#3</sup>,  $-x, y - 1, z + 1$ ; <sup>#4</sup>,  $-x + 1, y, -z + 1/2$ ; <sup>#5</sup>,  $-x + 1, y, -z + 3/2$ .

from 2.8 g ( $1.5 \times 10^{-2}$  mol) of ferrocene, in hexane (150 mL) at room temperature. The reaction mixture was stirred for 3 days at room temperature; then, the resulting brown suspension was evaporated to dryness, and the mixture redissolved in diethyl ether (100 mL). The organic phase was washed with water (100 mL  $\times$  3) and dried over MgSO<sub>4</sub>. After evaporation of the solvent, the product was separated by column chromatography on silica gel. Elution with dichloromethane yielded a reddish-orange fraction containing **L2** in a 6% yield (0.24 g). Crystals of **L2** suitable for single-crystal X-ray analysis were obtained by slow evaporation of a pentane solution at ambient temperature. <sup>1</sup>H NMR (400 MHz, CDCl<sub>3</sub>, 25 °C, TMS, ppm)  $\delta$ : 8.69 (d, 1H,  $J_{\text{HH}} = 3.5$  Hz), 8.43 (m, 1H), 8.32 (m, 1H), 4.96 (m, 2H), 4.49 (m, 2H), 4.08 (s, 5H). IR (KBr, cm<sup>-1</sup>): 3111 (w), 3081 (w), 3052 (w), 1577 (m), 1518 (s), 1498 (s), 1399 (s), 1386 (m), 1283 (m), 1138 (m), 1110 (m), 1030 (m), 1014 (m), 1002 (m), 847 (m), 837 (m), 830 (m), 812 (m), 519 (m), 496 (m), 481 (m), 475 (m). Anal. Calcd for C<sub>14</sub>H<sub>12</sub>N<sub>2</sub>Fe: C, 63.66; H, 4.58; N, 10.61. Found: C, 63.66; H, 4.27; N, 10.42.

**(L1)<sub>4</sub>·Ni(SCN)<sub>2</sub> (1a)**. To a solution of Ni(SCN)<sub>2</sub>·1/2H<sub>2</sub>O (4.5 mg,  $0.25 \times 10^{-2}$  mmol) in 2 mL of methanol was added a solution of **L1** (26 mg,  $1.0 \times 10^{-2}$  mmol) in 4 mL of methanol. After standing for a few days, orange crystals were formed in a 66% yield (20 mg), which were suitable for X-ray analysis. IR (KBr, cm<sup>-1</sup>): 3077 (m), 2067 (s), 1587 (m), 1555 (m), 1481 (m), 1404 (m), 1177 (m), 1003 (m), 892 (m), 822 (m), 715 (m), 510 (m), 491 (m), 474 (m). Anal. Calcd for C<sub>58</sub>H<sub>48</sub>N<sub>10</sub>Fe<sub>4</sub>NiS<sub>2</sub>: C, 56.58; H, 3.93; N, 11.38. Found: C, 56.41; H, 3.95; N, 11.36.

**(L1)<sub>4</sub>·Co(SCN)<sub>2</sub> (1b)**. This material was prepared as described for **1a** using **L1** (26 mg,  $1.0 \times 10^{-2}$  mmol) and Co(SCN)<sub>2</sub> (4.5 mg,  $0.25 \times 10^{-2}$  mmol). Reddish orange crystals were formed as a minor product, together with a powdered main product. The minor product was subjected to X-ray structure determination and confirmed to be the 4:1 complex, **(L1)<sub>4</sub>·Co(SCN)<sub>2</sub> (1b)**. The major product seem to be a 3:1 complex, **(L1)<sub>3</sub>·Co(SCN)<sub>2</sub>·H<sub>2</sub>O**. IR (KBr, cm<sup>-1</sup>): 3114 (w), 3072 (w), 2056 (s), 1635 (m), 1589 (m), 1562 (m), 1479 (m), 1404 (s), 1178 (m), 1003 (m), 816 (m), 715 (m),

490 (m), 471 (m). Anal. Calcd for C<sub>44</sub>H<sub>40</sub>N<sub>8</sub>OFe<sub>3</sub>CoS<sub>2</sub> (= **(L1)<sub>3</sub>·Co(SCN)<sub>2</sub>·H<sub>2</sub>O**): C, 53.63; H, 3.89; N, 11.37. Found: C, 53.54; H, 3.79; N, 11.36.

**(L1)<sub>3</sub>·Cu(NO<sub>3</sub>)<sub>2</sub> (2)**. This material was prepared as described for **1a** using **L1** (26 mg,  $1.0 \times 10^{-2}$  mmol) and Cu(NO<sub>3</sub>)<sub>2</sub>·3H<sub>2</sub>O (8 mg,  $0.3 \times 10^{-2}$  mmol). After standing for a few days, orange crystals were formed in a 35% yield (12 mg), which were suitable for X-ray analysis. IR (KBr, cm<sup>-1</sup>): 3014 (m), 1637 (m), 1562 (m), 1479 (s), 1407 (m), 1384 (s), 1297 (s), 1280 (m), 1004 (m), 829 (m), 713 (m), 514 (m), 489 (m), 472 (m). Anal. Calcd for C<sub>42</sub>H<sub>36</sub>N<sub>8</sub>Fe<sub>3</sub>O<sub>6</sub>Cu: C, 51.48; H, 3.70; N, 11.44. Found: C, 51.47; H, 3.68; N, 11.37.

**(L1)<sub>2</sub>·Cu(NO<sub>3</sub>)<sub>2</sub> (3)**. This material was prepared as described for **1a** using **L2** (26 mg,  $1.0 \times 10^{-2}$  mmol) and Cu(NO<sub>3</sub>)<sub>2</sub>·3H<sub>2</sub>O (12 mg,  $0.5 \times 10^{-2}$  mmol). After standing for a few days, dark green crystals were formed, which were suitable for X-ray analysis. The product was obtained in a 50% yield (19 mg). IR (KBr, cm<sup>-1</sup>): 3100 (w), 3084 (w), 1601 (m), 1523 (s), 1491 (s), 1406 (m), 1387 (s), 1268 (s), 1178 (m), 1143 (m), 1104 (m), 1008 (s), 853 (m), 817 (m), 747 (m), 510 (m), 480 (s), 418 (m). Anal. Calcd for C<sub>28</sub>H<sub>24</sub>N<sub>6</sub>O<sub>6</sub>CuFe<sub>2</sub>: C, 46.98; H, 3.38; N, 11.74. Found: C, 46.99; H, 3.19; N 11.25.

**(L1)<sub>2</sub>·Mn(hfac)<sub>2</sub> (4a)**. To a solution of **L1** (26 mg,  $1.0 \times 10^{-2}$  mmol) in 3 mL of diethyl ether was added a solution of Mn(hfac)<sub>2</sub>·2H<sub>2</sub>O (25 mg,  $0.5 \times 10^{-2}$  mmol) in 2 mL of diethyl ether. After standing for a few days, an orange crystalline solid of **3a** formed in a 69% yield (35 mg). IR (KBr, cm<sup>-1</sup>): 3114 (w), 3071 (w), 3039 (w), 1943 (w), 1878 (w), 1646 (s), 1566 (m), 1537 (m), 1486 (s), 1439 (m), 1407 (m), 1298 (m), 1256 (s), 1220 (s), 1176 (s), 1144 (s), 892 (m), 815 (m), 716 (m), 662 (s), 646 (m), 583 (m), 468 (m). Anal. Calcd for C<sub>38</sub>H<sub>26</sub>N<sub>4</sub>O<sub>4</sub>F<sub>12</sub>Fe<sub>2</sub>Mn: C, 45.77; H, 2.63; N, 5.62. Found: C, 45.75; H, 2.55; N, 5.41.

**(L1)<sub>2</sub>·Ni(hfac)<sub>2</sub> (4b)**. This material was prepared as described for **4a** using **L1** (26 mg,  $1.0 \times 10^{-2}$  mmol) and Ni(hfac)<sub>2</sub>·2H<sub>2</sub>O (25 mg,  $0.5 \times 10^{-2}$  mmol), yielding dark brown crystals, 72% yield (37 mg). IR (KBr, cm<sup>-1</sup>): 3107 (w), 3077 (w), 1946 (w), 1882 (w), 1644 (s), 1566 (m), 1534 (m), 1489 (s), 1438 (m), 1409 (m),

1257 (s), 1207 (s), 1177 (s), 1148 (s), 1001 (m), 826 (m), 811 (m), 715 (m), 671 (m), 588 (m), 491 (m), 472 (m). Anal. Calcd for  $C_{38}H_{26}N_4O_4F_{12}Fe_2Ni$ : C, 45.60; H, 2.62; N, 5.60. Found: C, 45.35; H, 2.26; N, 5.49.

**(L1)<sub>2</sub>·Cu(hfac)<sub>2</sub> (4c).** This material was prepared as described for **3a** using **L1** (26 mg,  $1.0 \times 10^{-2}$  mmol) and  $Cu(hfac)_2 \cdot H_2O$  (25 mg,  $0.5 \times 10^{-2}$  mmol), yielding orange-red crystals, 67% yield (34 mg). IR (KBr,  $cm^{-1}$ ): 3107 (w), 3065 (w), 1647 (s), 1590 (m), 1565 (m), 1534 (m), 1489 (s), 1458 (s), 1438 (m), 1409 (m), 1296 (m), 1258 (s), 1204 (s), 1176 (s), 1154 (s), 1001 (m), 893 (m), 812 (m), 714 (m), 669 (m), 586 (m), 508 (m), 491 (m), 469 (m). Anal. Calcd for  $C_{38}H_{26}N_4O_4F_{12}CuFe_2$ : C, 45.38; H, 2.61; N, 5.57. Found: C, 45.20; H, 2.64; N, 5.26.

**(L1)<sub>2</sub>·Zn(hfac)<sub>2</sub> (4d).** This material was prepared as described for **3a** using **L1** (26 mg,  $1.0 \times 10^{-2}$  mmol) and  $Zn(hfac)_2 \cdot 2H_2O$  (25 mg,  $0.5 \times 10^{-2}$  mmol), yielding orange crystals, 70% yield (36 mg). IR (KBr,  $cm^{-1}$ ): 3109 (w), 3077 (w), 1648 (s), 1566 (m), 1538 (m), 1489 (s), 1205 (s), 1205 (s), 1178 (m), 1147 (s), 1096 (m), 894 (w), 811 (m), 715 (m), 666 (m), 586 (m), 596 (w), 470 (w). Anal. Calcd for  $C_{38}H_{26}N_4O_4F_{12}Fe_2Zn$ : C, 45.29; H, 2.60; N, 5.56. Found: C, 45.56; H, 2.64; N, 5.56.

**(L2)<sub>2</sub>·Mn(hfac)<sub>2</sub> (5a).** To a solution of **L2** (26 mg,  $1.0 \times 10^{-2}$  mmol) in 3 mL of diethyl ether was added a solution of  $Mn(hfac)_2 \cdot 2H_2O$  (25 mg,  $0.5 \times 10^{-2}$  mmol) in 2 mL of diethyl ether. After standing for a few days, orange-red crystalline solids of **4a** formed in 85% yield (43 mg). IR (KBr,  $cm^{-1}$ ): 3286 (w), 3105 (m), 3091 (m), 1646 (s), 1591 (m), 1559 (m), 1532 (m), 1489 (s), 1404 (s), 1253 (m), 1223 (s), 1205 (s), 1150 (s), 1034 (m), 896 (w), 850 (m), 810 (m), 802 (m), 738 (m), 663 (m), 584 (m), 520 (w), 481 (m), 478 (m). Anal. Calcd for  $C_{38}H_{26}N_4O_4F_{12}Fe_2Mn$ : C, 45.77; H, 2.63; N, 5.62. Found: C, 45.43; H, 2.51; N, 5.39.

**(L2)<sub>2</sub>·Ni(hfac)<sub>2</sub> (5b).** This material was prepared as described for **5a** using **L2** (26 mg,  $1.0 \times 10^{-2}$  mmol) and  $Ni(hfac)_2 \cdot 2H_2O$  (25 mg,  $0.5 \times 10^{-2}$  mmol), yielding orange-red powder, 76% yield (39 mg). IR (KBr,  $cm^{-1}$ ): 3128 (w), 3098 (w), 3064 (w), 1644 (s), 1592 (m), 1558 (m), 1539 (m), 1486 (s), 1403 (m), 1341 (w), 1256 (s), 1206 (s), 1175 (s), 1140 (s), 1034 (m), 898 (w), 853 (m), 812 (m), 801 (m), 739 (w), 674 (s), 588 (m), 521 (m), 502 (m), 478 (m), 430 (w). Anal. Calcd for  $C_{38}H_{26}N_4O_4F_{12}Fe_2Ni$ : C, 45.60; H, 2.62; N, 5.60. Found: C, 45.56; H, 2.57; N, 5.44.

**(L2)<sub>2</sub>·Cu(hfac)<sub>2</sub> (5c).** This material was prepared as described for **5a** using **L2** (26 mg,  $1.0 \times 10^{-2}$  mmol) and  $Cu(hfac)_2 \cdot H_2O$  (25 mg,  $0.5 \times 10^{-2}$  mmol), yielding dark brown crystals, 51% yield (26 mg). IR (KBr,  $cm^{-1}$ ): 3120 (w), 3099 (w), 1661 (s), 1592 (m), 1552 (m), 1532 (m), 1521 (m), 1485 (s), 1404 (m), 1337 (w), 1260 (s), 1222 (s), 1177 (s), 1142 (s), 1070 (s), 1070 (m), 1034 (m), 852 (m), 808 (m), 800 (m), 729 (w), 668 (m), 592 (w), 577 (w), 522 (w), 502 (m), 484 (m). Anal. Calcd for  $C_{38}H_{26}N_4O_4F_{12}CuFe_2$ : C, 45.38; H, 2.61; N, 5.57. Found: C, 45.39; H, 2.49; N, 5.73.

**(L2)<sub>2</sub>·Zn(hfac)<sub>2</sub> (5d).** This material was prepared as described for **5a** using **L2** (26 mg,  $1.0 \times 10^{-2}$  mmol) and  $Zn(hfac)_2 \cdot 2H_2O$  (25 mg,  $0.5 \times 10^{-2}$  mmol), yielding yellow-orange powder, 78% yield (40 mg). IR (KBr,  $cm^{-1}$ ): 3138 (w), 3094 (w), 1646 (s), 1594 (m), 1559 (m), 1533 (m), 1486 (s), 1404 (m), 1254 (s), 1222 (s), 1203 (s), 1173 (s), 1135 (s), 1032 (m), 855 (m), 811 (m), 800 (m), 739 (w), 667 (m), 587 (m), 496 (m), 481 (m), 477 (m). Anal. Calcd for  $C_{38}H_{26}N_4O_4F_{12}Fe_2Zn$ : C, 45.29; H, 2.60; N, 5.56. Found: C, 45.38; H, 2.69; N, 5.56.

## Results and Discussion

### Ferrocene-Based Ligands, 5-Ferrocenylpyrimidine (**L1**) and Ferrocenylpyrazine (**L2**). 5-Ferrocenylpyrimidine (**L1**)

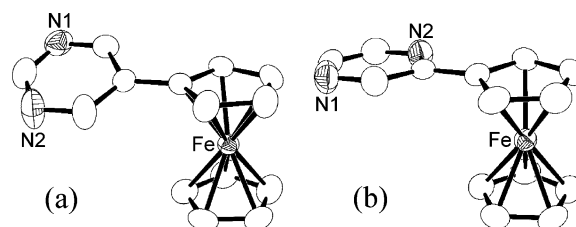


**Figure 1.** ORTEP representations (50% thermal probability ellipsoids) of the molecular structures of **L1** (a) and **L2** (b). Hydrogen atoms are omitted for clarity.

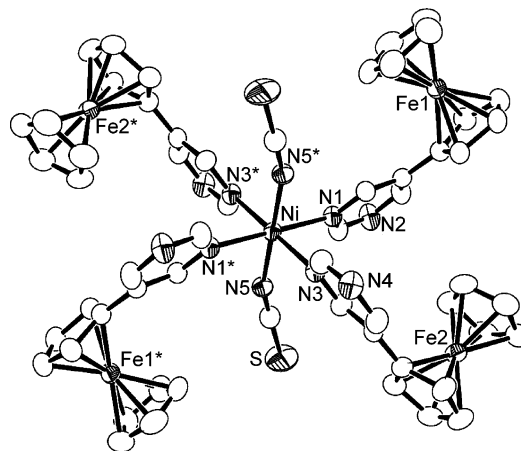


**Figure 2.** ORTEP representation (50% thermal probability ellipsoids) of the molecular structure of the 4:1 complex **1a** with the numbering scheme. Hydrogen atoms are omitted for clarity.

was synthesized by a palladium-catalyzed cross-coupling of zincated ferrocene with 5-bromopyrimidine, and ferrocenylpyrazine (**L2**) was prepared by the reaction of lithioferrocene with pyrazine (Scheme 1). ORTEP<sup>18</sup> drawings of these compounds are shown in Figure 1. The torsion angles between the cyclopentadienyl (Cp) ring and the heteroaryl ring are  $21.7(1)^\circ$  and  $7.8(1)^\circ$ , for **L1** and **L2**, respectively. The planarity of the latter may be ascribable to the decrease of steric hindrance of the ring hydrogen.

The cyclic voltammograms of **L1** and **L2** in dichloromethane show half-wave potentials ( $E_{1/2}$ 's) at 0.11 and 0.09 V (vs  $FeCp_2/FeCp_2^+$ ), respectively. The positive shifts relative to ferrocene are ascribable to the electron-withdrawing effect of the heteroaryl rings, and these values are comparable to other typical heteroaryl-substituted ferrocene derivatives.<sup>19</sup>

**Pinwheel-Like Complexes with 4:1 L/M Stoichiometry, (L1)<sub>4</sub>·M(SCN)<sub>2</sub> [M = Ni (**1a**), Co (**1b**)].** Reaction of **L1** with  $M(SCN)_2$  (M = Ni, Co) gave the 4:1 complexes  $(L1)_4 \cdot M(SCN)_2$ , which involve five metal ions. An ORTEP view of the pinwheel-like structure of **1a** (M = Ni) is shown in Figure 2, with the numbering scheme. Compound **1b** (M = Co) is isomorphous to **1a**. The coordination geometry around the nickel ion in **1a** is pseudo-octahedral, and four **L1** ligands and two thiocyanate anions are coordinated to the equatorial and axial positions, respectively. The bond lengths and angles

(18) ORTEP-3 for Windows: Farrugia, L. J. *J. Appl. Crystallogr.* **1997**, *30*, 565.

(19) Isaac, C. J.; Price, C.; Horrocks, B. R.; Houlton, A.; Elsegood, M. R. J.; Clegg, W. *J. Organomet. Chem.* **2000**, *598*, 248–253.

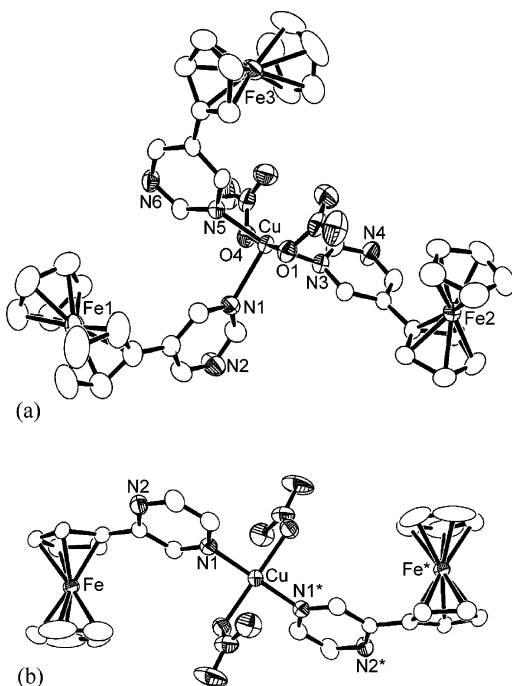


**Figure 3.** ORTEP representations (50% thermal probability ellipsoids) of the molecular structures of the 3:1 complex **2** (top, a) and the 2:1 complex **3** (bottom, b) with the numbering scheme. Hydrogen atoms are omitted for clarity.

around the Ni atom have normal values. The nickel atom lies on an inversion center, and thus, the unit contains two crystallographically independent **L1** ligands. Relative conformations of the two Cp rings in the ligands are synclinal (eclipsed), and the dihedral angles between the Cp ring and the pyrimidine ring are  $34.6(1)^\circ$  and  $14.5(1)^\circ$ , for **L1**(Fe1) and **L1**(Fe2), respectively.

**Copper(II) Complexes with Varying Stoichiometry,  $(\mathbf{L1})_3 \cdot \text{Cu}(\text{NO}_3)_2$  (**2**) and  $(\mathbf{L2})_2 \cdot \text{Cu}(\text{NO}_3)_2$  (**3**).** Reaction of **L1** with  $\text{Cu}(\text{NO}_3)_2$  gave the 3:1 complex  $(\mathbf{L1})_3 \cdot \text{Cu}(\text{NO}_3)_2$ , which involves four metal ions. An ORTEP view of this complex is shown in Figure 3a, with the numbering scheme. The coordination geometry around the copper ion is penta-coordinated, with the five donor atoms at the vertices of a distorted square pyramid formed by three **L1** ligands and two nitrate anions. The Cu–N(1) bond length of  $2.276(4)$  Å is slightly longer than the Cu–N(3) and Cu–N(5) of  $2.035(3)$  and  $2.036(3)$  Å, respectively, due to the Jahn–Teller effect. The Cu–O(1) and Cu–O(4) bond lengths are  $1.987(3)$  and  $1.979(3)$  Å, respectively, and there is no significant departure from planar coordination geometry within the  $\text{CuN}_2\text{O}_2$  unit. Conformations of the two Cp rings are synclinal (eclipsed) and located ca.  $1.63$ – $1.64$  Å away from the iron atom. The dihedral angles between the Cp ring and the pyrimidine ring are  $6.2(3)^\circ$ ,  $10.4(2)^\circ$ , and  $28.9(2)^\circ$ , for **L1**(Fe1), **L1**(Fe2), and **L1**(Fe3), respectively.

In contrast, reaction of **L2** with  $\text{Cu}(\text{NO}_3)_2$  produced a 2:1 complex  $(\mathbf{L2})_2 \cdot \text{Cu}(\text{NO}_3)_2$ , which involves three metal ions. An ORTEP view of this complex is shown in Figure 3b, with the numbering scheme. The copper(II) ion, which is located on an inversion center, adopts a square planar coordination geometry and is trans coordinated by two nitrate

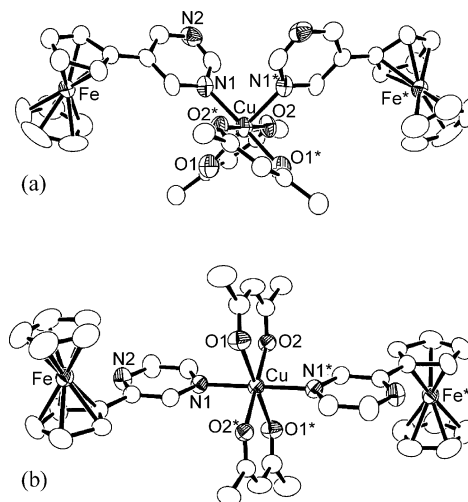


**Figure 4.** ORTEP representations (50% thermal probability ellipsoids) of the molecular structures of the cis 2:1 complex **4c** (top, a) and the trans complex **5c** (bottom, b) with the numbering scheme. Hydrogen and fluorine atoms are omitted for clarity.

anions and two **L2** ligands. The Cu–O(1) and Cu–N(1) distances are typical at  $2.007(3)$  and  $1.976(4)$  Å, respectively. The torsion angle between the Cp ring and the heteroaryl ring is  $26.3(2)^\circ$ , which is significantly larger than the value observed in the precursor **L2**.

**M(hfac)<sub>2</sub> Complexes with 2:1 L/M Stoichiometry,  $(\mathbf{L2})_2 \cdot \text{M}(\text{hfac})_2$  [ $\mathbf{L} = \mathbf{L1}$ ,  $\mathbf{M} = \text{Mn}$  (**4a**),  $\text{Ni}$  (**4b**),  $\text{Cu}$  (**4c**),  $\text{Zn}$  (**4d**);  $\mathbf{L} = \mathbf{L2}$ ,  $\mathbf{M} = \text{Mn}$  (**5a**),  $\text{Ni}$  (**5b**),  $\text{Cu}$  (**5c**),  $\text{Zn}$  (**5d**)].** Reaction of **L1** with  $\text{M}(\text{hfac})_2$  gave the 2:1 complexes,  $(\mathbf{L1})_2 \cdot \text{M}(\text{hfac})_2$  ( $\mathbf{M} = \text{Mn}$  (**4a**),  $\text{Ni}$  (**4b**),  $\text{Cu}$  (**4c**),  $\text{Zn}$  (**4d**)), which involve three metal ions. The molecular structure of **4c** is shown in Figure 4a. Compounds **4a**, **4b**, and **4d** are isomorphous to **4c**, and these complexes exhibited the cis configurations of the  $\text{M}(\text{hfac})_2$  unit. The metal center in  $\text{M}(\text{hfac})_2$  in **4c** has a slightly distorted tetrahedral coordination environment and shows no significant Jahn–Teller distortion with Cu–O(1), Cu–O(2), and Cu–N(1) bond lengths of  $2.109(5)$ ,  $1.983(5)$ , and  $2.184(6)$  Å, respectively. The bond lengths and bond angles of **4b** and **4d** around the metal centers are almost the same as those found in **4c** (Table 3). The dihedral angles between the Cp ring and the pyrimidine ring in the **L1** ligands in **4b** ( $\mathbf{M} = \text{Ni}$ ), **4c** ( $\mathbf{M} = \text{Cu}$ ), and **4d** ( $\mathbf{M} = \text{Zn}$ ) are  $20.9(2)^\circ$ ,  $18.7(3)^\circ$ , and  $17.6(2)^\circ$ , respectively, which are similar to the value found in the precursor **L1**.

Reaction of **L2** with  $\text{M}(\text{hfac})_2$  also produced 2:1 complexes,  $(\mathbf{L2})_2 \cdot \text{M}(\text{hfac})_2$  ( $\mathbf{M} = \text{Mn}$  (**5a**),  $\text{Ni}$  (**5b**),  $\text{Cu}$  (**5c**),  $\text{Zn}$  (**5d**)). However, the coordination structures exhibit trans configurations, in contrast to **4a**–**d**. The molecular structure of **5c** is shown in Figure 4b. The copper atom lies on an inversion center, and each N-donor ligand occupies the trans positions relative to the copper(II) ions. Elongation of Cu(1)–O(1) ( $2.300(3)$  Å) relative to Cu(1)–O(2) ( $1.964(2)$  Å) is ascribable to the Jahn–Teller effect. The dihedral angle between the Cp ring and the pyrimidine ring in ligand **L2** in **5c** is  $3.7(1)^\circ$ , which is similar to the value observed in the precursor **L2**. Intermolecular magnetic interactions in these *molecular* complexes are expected to be negligibly small due to long intermolecular metal–metal distances.

**Table 4.** Dihedral Angles (deg) between Cyclopentadienyl Ring and Heteroaryl Ring in **L1**, **L2**, and Ligands in Metal Complexes

compd	torsion angle	compd	torsion angle
<b>L1</b>	21.7(1)	<b>L2</b>	7.8(1)
<b>1a</b>	14.5(1), 34.6(1)	<b>2</b>	6.2(3), 10.4(2), 28.9(2)
<b>3</b>	26.3(2)	<b>4b</b>	20.9(2)
<b>4c</b>	18.7(3)	<b>4d</b>	17.6(2)
<b>5c</b>	3.7(1)		

**Discussion of the Coordination Structure.** In this study, we have synthesized a series of metal-centered polynuclear complexes by using the simple ferrocene-based ligands **L1** and **L2**. In these complexes, both ligands act as monodentate ligands, leaving one of the two nitrogens free. The poor coordination ability of the 1-nitrogen (N2) in **L2** may be accounted for by the steric hindrance of the adjacent ferrocenyl group, whereas a free pyrazine molecule can link metal ions to produce multinuclear compounds or coordination polymers.<sup>10</sup> The dihedral angles between the Cp ring and the arene ring of the present compounds are listed in Table 4. The smaller dihedral angle in **L2** relative to that in **L1** may be ascribable to the smaller steric hindrance, although variation of the angles as seen in Table 4 indicates that these angles are rather flexible. On the other hand, **L1** is expected to act also as a bidentate ligand. Indeed, as reported in a separate paper, **L1** also affords coordination polymers,  $\{\mathbf{L1}\cdot\mathbf{M}(\text{hfac})_2\}_n$  ( $\mathbf{M} = \text{Mn, Ni, Cu, Zn}$ ) and  $\{\mathbf{L1}\cdot\text{CuX}\}_n$  ( $\text{X} = \text{I, Br}$ ), in which the ligand acts as a bridging ligand.<sup>11</sup> In the present study, we could selectively synthesize the polynuclear complexes by recrystallization from diethyl ether, whereas reactions of **L1** with equimolar amounts of  $\text{M}(\text{hfac})_2$  in heptane produced the 1:1 coordination polymers.

The stoichiometric and structural differences as observed in these polynuclear complexes may be the consequence of competition or synergy between the steric factors inside the complexes and packing effects upon crystallization. The followings points should be noted on the stoichiometry and the structures of the present complexes: (i) the ligand **L1** produced 4:1 complexes (**1a**, **1b**), a 3:1 complex (**2**), and 2:1 complexes (**4a–4d**), whereas **L2** produced only 2:1 complexes (**3**, **5a–5d**); (ii) reaction of  $\text{Cu}(\text{NO}_3)_2$  with **L1** produced a 3:1 complex, whereas that with **L2** produced a 2:1 complex; and (iii) concerning  $\text{M}(\text{hfac})_2$  complexes, we could only isolate cis complexes for **L1** and trans complexes for **L2**, regardless of the metal species. We found that the M/L ratio of the present compounds was not affected by changes in the stoichiometry of metal salts and the ligands used in the reaction, although typical experimental conditions are described in the Experimental Section. It is interesting to note that the coordination polymers of  $\{\mathbf{L1}\cdot\mathbf{M}(\text{hfac})_2\}_n$  exhibit the cis configurations of the  $\text{M}(\text{hfac})_2$  unit, whereas the molecular complexes of  $(\mathbf{L1})_2\cdot\text{M}(\text{hfac})_2$  display the trans ones. The difference in the shapes of **L1** and **L2**, under the influence of packing effects, may have resulted in the stabilization of these different coordination modes in the crystals. As related ligands, the pyridyl ferrocenes (pyfc)<sup>20</sup> have been known for many years, but only a few of their coordination complexes have been reported; Laguna and co-workers demonstrated that complexation of 3-pyfc with  $\text{Au}^{\text{I}}$

**Table 5.** Redox Potentials from Cyclic Voltammetry (in V vs  $\text{FeCp}_2/\text{FeCp}_2^+$ )

compd	$E_{1/2}$	$E_{pc}$	$E_{pa}$	compd	$E_{1/2}$	$E_{pc}$	$E_{pa}$
<b>L1</b>	0.10	0.31	−0.11	<b>L2</b>	0.11	0.31	−0.08
<b>1a</b>	0.05	0.10	0.00	<b>1b</b>	0.06	0.20	−0.09
<b>2</b>	<i>a</i>		−0.12	<b>3</b>	<i>a</i>		−0.18
<b>4a</b>	0.05	0.10	0.00	<b>4b</b>	0.05	0.13	0.02
<b>4c</b>	0.07	0.13	0.02	<b>4d</b>	0.07	0.15	0.00
<b>5a</b>	0.08	0.17	−0.01	<b>5b</b>	0.07	0.11	0.03
<b>5c</b>	0.09	0.14	0.04	<b>5d</b>	0.07	0.14	0.01

<sup>a</sup> Irreversible.

and  $\text{Au}^{\text{III}}$  ions produce 1:1 and 2:1 complexes, respectively.<sup>21</sup> Interestingly, the assembled structures of these complexes and the present ones are quite different, although the coordination modes of **L1**, **L2**, and 3-pyfc appear to be similar. On the other hand, 2-pyfc rarely produce coordination compounds except when ortho-metalation<sup>19,22</sup> occurs, although chelate complexes are reported for 1,1'-(2-pyridyl)-ferrocene and its analogues.<sup>23</sup>

**Solid-State Electrochemistry.** Cyclic voltammograms of these complexes were measured in the solid state. Solid-state redox potentials of the present compounds are listed in Table 5. Compounds **L1** and **L2** show half-wave potentials at  $E_{1/2} = 0.10$  and 0.11 V (vs solid-state  $\text{FeCp}_2/\text{FeCp}_2^+$ ), respectively, which are slightly shifted from those in solution. As listed in Table 5, the  $E_{1/2}$  values for **4a–4d** are observed at around 0.06 V, whereas those of **5a–5d** are observed at around 0.08 V, which corresponds to the redox process of the ferrocenyl moiety. These potentials show negative shifts with respect to those of **L1** and **L2** in the solid state; lowering of the redox potentials in the metal complexes is probably due to electrostatic stabilization between the resultant ferrocenium ions and neighboring anionic moieties, as generally observed in the ionization processes of molecular solids.<sup>24</sup> Similar tendencies have been reported for the redox processes of  $[\text{M}(\text{hfac})_2\{1,1'\text{-di}(\text{pyridinethio})\text{ferrocene}\}]_n$  ( $\text{M} = \text{Mn, Cu, Zn}$ ).<sup>5</sup> In addition to the redox waves of the ferrocenyl groups, the copper derivatives **4c** and **5c** show another redox wave at  $E_{1/2} \sim -0.2$  V in the solid state. This is assignable to a redox process involving the  $\text{Cu}(\text{hfac})_2$  unit, because the  $\text{Cu}(\text{hfac})_2\cdot n\text{H}_2\text{O}$  complex shows a redox peak at around  $-0.30$  V in the solid state, whereas those of  $\text{M} = \text{Mn, Ni, and Zn}$  show no significant redox waves in the range  $-0.6$  to 0.5 V. It is interesting to know whether electronic communication<sup>25</sup> occurs between the ferrocenyl groups through

- (20) (a) Rausch, M. D.; Ciappenelli, D. J. *J. Organomet. Chem.* **1967**, *10*, 127–136. (b) Carugo, O.; De Santis, G.; Fabbrizzi, L.; Licchelli, M.; Monichino, A.; Pallavicini, P. *Inorg. Chem.* **1992**, *31*, 765–769. (c) Liu, C.-M.; Chen, B.-H.; Liu, W.-Y.; Wu, X.-L.; Ma, Y.-X. *J. Organomet. Chem.* **2000**, *598*, 348–352.
- (21) Barranco, E. M.; Crespo, O.; Gimeno, M. C.; Jones, P. G.; Laguna, A.; Villacampa, M. D. *J. Organomet. Chem.* **1999**, *592*, 258–264.
- (22) Yoshida, T.; Tani, K.; Yamagata, T.; Tatsuno, Y.; Saito, T. *J. Chem. Soc., Chem. Commun.* **1990**, 292–294.
- (23) (a) Tani, K.; Mihana, T.; Yamagata, T.; Saito, T. *Chem. Lett.* **1991**, 2047–2050. (b) Delis, J. G. P.; van Leeuwen, P. W. N. M.; Vrieze, K.; Veldman, N.; Spek, A. L.; Fraanje, J.; Goubitz, K. *J. Organomet. Chem.* **1996**, *514*, 125–136. (c) Neumann, B.; Siemeling, U.; Stammer, H.-G.; Vorfeld, U.; Delis, J. G. P.; van Leeuwen, P. W. M. N.; Vrieze, K.; Fraanje, J.; Goubitz, K.; de Biani, F.; Zanella, P. *J. Chem. Soc., Dalton Trans.* **1997**, 4705–4711.
- (24) *The Electronic Structure and Chemistry of Solids*; Cox, P. A.; Oxford University Press: New York, 1987.

the metal centers. However, the present complexes dissociate in usual organic solvents, and thus, we measured solid-state voltammograms of the bulk materials, from which we could not obtain detailed information on individual electrochemical processes.

It should be noted that the redox potentials of these heteroaryl ferrocenes are lower than those of dppf or bis-pyridinethio ferrocenes by ca. 0.1 and 0.4 V, respectively.<sup>5,26</sup> The lower redox potentials of the monosubstituted ligands are advantageous when producing coordination compounds involving ferrocenium cations by electrochemical oxidation.

## Conclusion

We have designed simple ferrocene-based ligands with pyrimidine or pyrazine moieties and obtained electroactive polynuclear complexes with varying L/M stoichiometry. These polynuclear complexes can be regarded as metal-centered ferrocene clusters, although there are several other interesting examples of ferrocene-based assemblies.<sup>8,9,12,27</sup>

- (25) Hendrickson, D. N. *Mixed Valency Systems: Applications in Chemistry, Physics, and Biology*; Prassides, K., Ed.; Kluwer: Dordrecht, 1991.
- (26) Yamamoto, Y.; Tanase, T.; Mori, I.; Nakamura, Y. *J. Chem. Soc., Dalton Trans.* **1994**, 3191–3192.
- (27) (a) Niu, Y.-Y.; Chen, T.-N.; Liu, S.-X.; Song, Y.-L.; Wang, Y.-X.; Xue, Z.-L.; Zin, X.-Q. *J. Chem. Soc., Dalton Trans.* **2002**, 1980–1984. (b) Cai, Y.; Song, Y.; Zheng, H.; Niu, Y.; Du, C.; Xin, X. *Chem. Lett.* **2002**, 508–509.

Through the present and related studies,<sup>11,28</sup> the ligand design has been shown to be useful for synthesizing ferrocene-based coordination compounds. These ligands may be also useful for the construction of ferrocene-based organometallic dendrimers,<sup>29</sup> and a study is underway in our laboratories.

**Acknowledgment.** This work was supported by the Morino Foundation for Molecular Science. We acknowledge JST (Japan Science and Technology Corporation) for the loan of experimental equipment. We are grateful to Mr. Z. He (Toho University) for his help with powder X-ray diffraction measurements. We also thank Mr. M. Nakama (WarpStream Ltd., Tokyo) for constructing Web-DB systems, and Mr. M. Itou (Toho University) for his help with searching online databases.

**Supporting Information Available:** Crystallographic data in CIF format. This material is available free of charge via the Internet at <http://pubs.acs.org>.

IC034684Y

- (28) Horikoshi, R.; Nambu, C.; Mochida, T. *New J. Chem.*, in press.
- (29) (a) Astruc, D. *Acc. Chem. Res.* **2000**, *33*, 287–298. (b) Casado, C. M.; Cuadrado, I.; Morán, M.; Alonso, B.; García, B.; Gozález, B.; Losada, J. *Coord. Chem. Rev.* **1999**, *186*, 53–80. (c) Nlate, S.; Ruiz, J.; Sartor, V.; Navarro, R.; Blais, J. C.; Astruc, D. *Chem. Eur. J.* **2000**, *6*, 2544–2553. (d) Turrin, C.-O.; Chiffre, J.; de Montauzon, D.; Daran, J.-C.; Caminade, A. M.; Manoury, E.; Balavoine, G.; Majoral, J. P. *Macromolecules* **2000**, *33*, 7328–7336. (e) Palomero, J.; Mata, J. A.; González, F.; Peris, E. *New J. Chem.* **2002**, *26*, 291–297.